

Analysis of low pressure electro-positive and electro-negative rf plasmas with Monte Carlo method

M. Ardehali ¹

Silicon Systems Research Laboratories, NEC Corporation,
Sagamihara, Kanagawa 229 Japan

Abstract

Particle-in-cell/Monte Carlo technique is used to simulate low pressure electro-negative and electro-positive plasmas at a frequency of 10 MHz. The potential, electric field, electron and ion density, and currents flowing across the plasma are presented. To compare the physical properties of the electro-positive gas with those of an electro-negative gas, the input voltage was decreased from 1000 Volts to 350 Volts. The simulation results indicate that the introduction of negative ions induces dramatic effects on the spatial and temporal variation of the electric field and on the behavior of the electron, ion, and displacement currents. In particular, the numerical modeling predicts the formation of double-layer at the plasma-sheath boundary of electro-negative discharge.

¹email: ardehali@apexmail.com

I. Introduction

Plasma-assisted processing is becoming increasingly important in microelectronics industry [1]. The figures-of-merit of the process (for example anisotropy, etching rate, etc.) are strongly influenced by the discharge properties, such as plasma density, plasma potential, etc [2], [3]. Obviously predictive models are needed to analyze the rf glow discharges [4]. Unfortunately, plasma discharges are complex systems that are very difficult to analyze. In recent years, there has been considerable efforts to model these systems self-consistently. Particle-in-cell/Monte-Carlo (PIC/MC) simulation has proven to be an effective and powerful tool in increasing the general understanding of plasma processing. PIC/MC simulation is very attractive because it has the advantage of being self-consistent and does not require any assumptions regarding the internal electric field, the electron velocity distribution function, and the relaxation time approximation [5].

The purpose of the present paper is to compare the physical properties of an electro-positive gas with those of an electro-negative gas at comparable plasma densities. The simulation results indicate that the introduction of negative ions in rf plasma induces dramatic effects on the electric field distribution within the discharge and leads to the double-layer formation.

II. Details of simulation

We have developed a PIC/MC simulator to model electro-positive and electro-negative discharges. Monte Carlo technique is considerably more accurate than fluid dynamics method because it accounts for the non-local effects naturally; whereas fluid dynamics accounts for the non-local effects on an *ad hoc* basis.

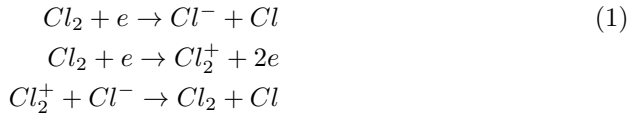
Very briefly, the present PIC/MC simulator consists of the following steps:

- (1) The instantaneous locations of MC particles representing ions and electrons are interpolated to the grid points to obtain the charge density.
- (2) Poisson's equation on a spatially discretized mesh is solved to obtain the electric field.
- (3) The electric field is interpolated from the grid points to the location of MC particles.
- (4) The equations of motion under the local and instantaneous electric field are integrated.
- (5) Random numbers (Monte Carlos technique) and collision cross sections are used to determine the probability that each particle suffers a collision.

As an example of the application of this simulator, we have modeled an rf plasma at a pressure of 20 mTorr. Since in this work we are primarily interested in comparing the physical properties of the electro-positive and electro-negative gases, we have intentionally kept the plasma model simple. In the simulation, the applied frequency is $\frac{\omega}{2\pi} = 10$ MHz, and the discharge length is 20 cm with perfectly absorbing electrodes. The time step $\delta t = 0.1$ ns which is small enough

to resolve the electron plasma frequency. For the electro-positive plasma, an Argon type discharge was considered. The left electrode of the discharge is driven with a voltage $V_{rf}(t) = V_{rf} \sin \omega t$, where $V_{rf} = 1000$ Volts. The electron-neutral ionization cross section $\sigma(v)$ is given by $\sigma(v) = \frac{k}{v}$, where v is the electron velocity and the rate constant k is $2 \times 10^{-8} \text{ cm}^3/\text{s}$. Ionizing collisions occur if the electron energy is larger than 15 eV. An ionizing collision is modeled by loading a new electron and ion at the position of the ionizing electron. The kinetic energy after ionizing collision is partitioned between the two electrons with equal probability.

For the electro-negative discharge, a Chlorine gas was considered. The left electrode of the discharge is driven with a voltage $V_{rf}(t) = V_{rf} \sin \omega t$, where $V_{rf} = 350$ Volts. The ionization cross section is the same as for the electro-positive gas. The additional processes considered are dissociative electron attachment leading to negative ion formation and positive ion/negative ion recombination. The scattering and ionization processes are represented as follows:



where Cl_2^+ and Cl^- are the main positive and negative ions, respectively. The rate constants for attachment and recombination are $1.8 \times 10^{-10} \text{ cm}^3/\text{s}$ and $5 \times 10^{-8} \text{ cm}^3/\text{s}$ respectively [6]. In the electro-negative discharge, the electron density is an order of magnitude smaller than the positive (or negative) ion density; in the simulation, however, the electron weight was adjusted to make the number of MC particles corresponding to electrons similar to the number of MC particles corresponding to positive and negative ions.

III. Electro-positive discharge

We first present the simulation results for an electro-positive discharge at a pressure of 20 mTorr. Figures 1(a) and 1(b) show the potential and the electric field at four times during the rf cycle. In the bulk, the potential is constant, and hence the electric field is negligible. In the sheath, however, the potential changes rapidly (due to accumulation of positive charge in the space charge region), and the electric field therefore becomes very large, especially near the electrodes. This is particularly evident at $\frac{\omega t}{2\pi} = 0.25$ and $\frac{\omega t}{2\pi} = 0.75$. Figures 2(a) and 2(b) show the ion and electron density of the electro-positive plasma. The ion density is independent of the phase of the applied voltage, whereas the electron density oscillates within the sheath. The large electric field at the sheath pushes the electrons away from the sheath, whereas it accelerates some of the positive ions toward the electrodes.

Figures 3(a), 3(b), 3(c), and 3(d) show the spatial and temporal variations of the electron current, displacement current, ion current, and total current at

four times during the cycle respectively (the units are not relative and represent true values). At $\frac{\omega t}{2\pi} = 0$ and $\frac{\omega t}{2\pi} = 0.5$, the sheath current is predominantly displacement current, whereas at $\frac{\omega t}{2\pi} = 0.25$ and ($\frac{\omega t}{2\pi} = 0.75$) the electron current is the dominant current in the sheath of the powered (grounded) electrode. The electron current, however, is dominant in the bulk at all times during the cycle. Since the bulk electric field does not change with time, the displacement current has a negligible value in the bulk. Also note that the bulk ion current (Fig. 3 (c)) does not modulate with time, but at the sheath boundary, the ion current increases abruptly due to the large sheath electric field and oscillates with time. The total current, which is defined as the sum of the electron, displacement and ion current (Fig. 3 (d)), is constant across the discharge.

IV. Electro-negative discharge

To obtain an electro-negative discharge with plasma density comparable to that of the electro-positive discharge, the applied voltage was decreased from 1000 Volts to 350 Volts. Figure 4(a) shows the potential at four times during the rf cycle. The potential changes significantly near the electrodes, leading to large electric fields within the sheaths. However unlike the electro-positive plasma, the potential in the bulk is not constant. Figure 4(b) shows the electric field profile at four times during the cycle. Since negative ions and electrons are excluded from the sheath, the space charge within the sheath is positive. Note that at times $\frac{\omega t}{2\pi} = 0.25$ and $\frac{\omega t}{2\pi} = 0.75$ the electric field becomes very large near the electrodes.

Comparing Figs. 1 (b) and 4 (b), three important differences between the electro-positive and electro-negative discharges may be noted:

- (1) Unlike the electro-positive discharge, the electric field has a nonvanishing value in the bulk of the electro-negative discharge.
- (2) In electro-negative discharge, the electric field shows a relative maximum at the plasma-sheath boundary. The maximum is due to double-layer formations and is particularly important at $\frac{\omega t}{2\pi} = 0$ and $\frac{\omega t}{2\pi} = 0.5$. This result is in agreement with experimental measurements [7].
- (3) The magnitude of the sheath electric field is significantly larger in the electro-positive discharge than in the electro-negative plasma.

These factors have profound influence on the behavior of the spatial and temporal variations of the electron, ion, and displacement currents within the discharge.

Figures 5(a) and 5(b) show the positive and negative ion density within the discharge. The ion density is independent of the phase of the applied voltage. The large electric field at the sheath pushes the negative ions away from the sheath and hence negative ions are completely excluded from the sheath. However, some of the positive ions are accelerated by the sheath toward the electrodes. It should be noted that in the bulk, negative ions are lost due to

recombination and hence do not accumulate at the boundary of the sheath and the glow region. Figure 5(c) shows the electron density at four times during the cycle. Unlike the ions, the electron density is a function of time and varies significantly within the sheath. When the sheath electric field at the left electrode is small, electrons move toward the left electrode but are excluded from the right electrode. On the other hand when the sheath electric field at the right electrode is small, electrons move toward the right electrode but are excluded from the left electrode. The modulation of the bulk electron density, however, is small and almost negligible. Fig. 5(d) compares the electron, positive ion and negative ion density at four times during the cycle. Note that in the bulk, the sum of the electron density and negative ion density is approximately equal to the positive ion density and hence total charge within the bulk is almost zero.

Figures 6(a), 6(b), 6(c), 6(d), and 6(e) show the spatial and temporal variations of the electron current, displacement current, positive ion current, negative ion current, and total current at four times during the cycle respectively (again, the units are not relative and represent true values). Similar to the electro-positive discharge, at $\frac{\omega t}{2\pi} = 0$ and $\frac{\omega t}{2\pi} = 0.5$ the sheath current is predominantly displacement current, whereas at $\frac{\omega t}{2\pi} = 0.25$ ($\frac{\omega t}{2\pi} = 0.75$) the electron current is the dominant current in the sheath of the powered (grounded) electrode. The electron current is dominant in the bulk at all times during the cycle. Note that the displacement current within the bulk is not zero and contributes to the total current. The non-vanishing of the bulk displacement current is primarily due to temporal variation of bulk electric field [see Fig. 4(b); the displacement current $J_d(t)$ is defined as $J_d(t) = -\epsilon_0(dE/dt)$]. The positive ion current across the discharge is shown in Fig. 6(c). The positive ion current increases only slightly at the sheath boundary. Comparing Figs. 3 (c) and 6 (c), one can see that in the electro-negative discharge, the ion current in the bulk varies with time (this is primarily due to temporal variation of the bulk electric field), and has a smaller modulation within the sheath. Fig. 6(d) shows the negative ion current across the discharge. Since negative ions are confined to the bulk of the plasma, the current within the sheath is negligible. However, in the bulk, the negative ion current oscillates with the applied voltage. Note the small contribution of positive and negative ion currents to the total current. Finally Fig. 6(e) shows the total current, which is defined as sum of the electron, positive and negative ion, and displacement current across the discharge. Although there is a small blip at the sheath boundary, the total current within the discharge is constant (experience has shown that the blip diminishes by increasing computation time).

It is worth noting that although plasma density in the two cases are comparable, the total current (as well as the electron, ion and displacement current) is approximately three times smaller in the electro-negative discharge than the corresponding currents in the electro-positive plasma.

V. Conclusion

In summary, we have presented the PIC/MC simulation results of an electro-positive and an electro-negative discharge at comparable plasma densities. The numerical results indicate that the presence of negative ions leads to a relative maximum at the plasma-sheath boundary, i.e., to the formation of double layers. This result is in agreement with the experimental measurements. The simulation results also indicate that unlike the electro-positive discharge, the bulk electric field of the electro-negative plasma has a nonvanishing value and oscillates with time. This oscillation leads to significant bulk displacement current and to modulation of bulk positive ion current.

Simulation results such as the ones reported here show great promise in interpreting experimental measurements and in testing the validity of analytical models and simulation models based on fluid dynamics. Future experiments, in conjunction with similar Monte Carlo simulations, can provide considerable information about the details of rf discharges and about the formation of double-layers.

References

- [1] D. M. Manson and D. L. Flamm, *Plasma Etching* (Academic, New York, 1989) p, 12.
- [2] R. A. Gottscho, C. J. Jurgensen, and D. J. Vitkavage, "Microscopic uniformity in plasma etching," *J. Vac. Sci. Technol. B*, vol. 10, pp. 2133-2147, 1992.
- [3] M. Ardehali, "Monte Carlo simulation of ion transport through radio frequency collisional sheath," *J. Vac. Sci. Technol. A* vol. 12, pp. 3242-3245, 1994; M. Ardehali, "Effect of image force on ion current density in plasma discharges", *IEEE Trans. Plasma Sci.*, vol. 24, pp. 241-245, 1996.
- [4] E. Gogolides, J. P. Nicolai, and H. H. Sawin, "Comparison of experimental measurements and model predictions for radio-frequency Ar and SF_6 discharges," *J. Vac. Sci. Technol. A*, vol. A7, no. 3, pp. 1001-1005, 1989; E. Gogolides, and H. H. Sawin, "Continuum modeling of radio-frequency glow discharges. I. Theory and results for electropositive and electronegative gases," *J. Appl. Phys.*, vol 72, pp. 3971-3987, 1992; E. Gogolides, and H. H. Sawin, "Continuum modeling of radio-frequency glow discharges. II. Parametric studies and sensitivity analysis," *J. Appl. Phys.*, vol 72, pp. 3988-4002, 1992.
- [5] D. Vender and R. W. Boswell, "Numerical modeling of low-pressure rf plasmas," *IEEE Trans. Plasma Sci.*, vol. 18, pp 725-732, 1990; M. Surendra and D. B. Graves, "Particle simulation of rf glow discharges," *IEEE Trans. Plasma Sci.*, vol. 19, pp. 144-157, 1990.
- [6] G. L. Ragoff, J. M. Kramer, and R. B. Piejak, *IEEE Trans. Plasma Sci.*, vol.14, pp. 103, 1986. **30**, 641, 1959.
- [7] R. A. Gottscho and C. E. Gaebe,"Negative ion kinetics in RF glow discharges," *IEEE Trans. Plasma Sci.* vol. 14, pp. 92-102, 1986. R. A. Gottscho and M. L. Mandich *J. Vac. Sci. Tech Vol. A* vol. 3, pp. 617, 1985; R. A. Gottscho, "Glow-discharge sheath electric field: Negative ion, power, and frequency effects," *Phys. Rev. A* vol. 36, pp. 2233-2242, 1987.

Important Note: All figures should be considered from left to right.

Figures 1 (a), 1 (b), 2 (a), and 2 (b) are on the same page.

Figures 3 (a), 3 (b), 3 (c), and 3 (d) are on the same page.

Figures 4 (a) and 4 (b) are on the same page.

Figures 5 (a), 5 (b), 5 (c), and 5 (d) are on the same page.

Figures 6 (a), 6 (b), 6 (c), 6 (d), and 6 (e) are on the same page.

Figure 1(a)- The spatial and temporal variations of the potential in the discharge. For Figs. 1 (a) to 3 (d), the discharge is electro-positive. All figures represent profiles at four times during the rf cycle: $\frac{\omega t}{2\pi} = 0$ (solid line), $\frac{\omega t}{2\pi} = 0.25$ (dotted line), $\frac{\omega t}{2\pi} = 0.5$ (dashed-dashed line), $\frac{\omega t}{2\pi} = 0.75$ (dashed line). the electro-negative gas

Figure 1(b)- The electric field profile.

Figure 2(a)- The positive ion density.

Figure 2(b)- The electron density.

Figure 3(a)- The spatial and temporal variations of the electron current across the discharge.

Figure 3(b)- Same as Fig 3 (a) but for the displacement current.

Figure 3(c)- Same as Fig 3 (a) but for the ion current.

Figure 3(d)- The spatial and temporal variations of the total current across the discharge.

Figure 4(a)- The potential profile in the discharge. For Figs. 4 (a) to 6 (e), the discharge is electro-negative.

Figure 4(b)- The electric field profile.

Figure 5(a)- The positive ion density.

Figure 5(b)- The negative ion density.

Figure 5(c)- The electron density.

Figure 5(d)- The positive ion, negative ion, and electron density.

Figure 6(a)- The spatial and temporal variations of the electron current across the discharge.

Figure 6(b)- Same as Fig 6 (a) but for the displacement current.

Figure 6(c)- Same as Fig 6 (a) but for the positive ion current.

Figure 6(d)- Same as Fig 6 (a) but for the negative ion current.

Figure 6(e)- The spatial and temporal variations of the total current across the discharge.

